

# Structural Insights into a Novel Molecular-Scale Composite of Soluble Poly(vinyl pyrrolidone) Supporting Uniformly Dispersed Nanoscale Poly(vinyl pyrrolidone) Particles

David K. Hood, Laurence Senak, Steven L. Kopolow, Michael A. Tallon, Yoon Tae Kwak, Drupesh Patel, John McKittrick

International Specialty Products, 1361 Alps Road, Wayne, New Jersey 07470

Received 2 July 2002; accepted 23 September 2002

**ABSTRACT:** Structural insights into a novel, molecular-composite poly(vinyl pyrrolidone) consisting of a soluble, film-forming poly(vinyl pyrrolidone) (PVP) polymer and *in situ* formed, minute, crosslinked, nanoscale, insoluble poly[poly(vinyl pyrrolidone)] (PPVP) polymer particles are reported. A technique for determining the PVP molecular weight and PPVP weight fraction by gel permeation chromatography/multi-angle light scattering (MALS) is described. Particle size studies by quasi-elastic light scattering and field flow fractionation/MALS demonstrate that the nanoscale, insoluble polymer particles are nominally 370 and 325 nm in diameter, respectively. Rheological experi-

ments on this dispersed system yield a complex macroscopic behavior. Atomic force microscopy images confirm a substantial heterogeneous nature for a film cast from this molecular-composite material. Finally, this polymeric molecular composite in film form exhibits, among many other interesting properties, a dramatic enhancement in water resistance, as demonstrated by a simple image water resistance test for an ink-jet printing application. © 2003 Wiley Periodicals, Inc. *J Appl Polym Sci* 89: 734–741, 2003

**Key words:** water-soluble polymers; nanotechnology; film forming; poly(vinyl pyrrolidone)

## INTRODUCTION

Commercial products of soluble poly(vinyl pyrrolidone) (PVP) or insoluble, crosslinked poly[poly(vinyl pyrrolidone)] (PPVP) have been available for more than 40 years. During this period, these materials have experienced great commercial growth and acceptance in a wide range of applications ranging from the detergent binding of fugitive dyes and ink/dye-receptive printable coatings to disintegrant enhancers, beverage clarifiers, and pharmaceutical excipients.<sup>1</sup> There continues to be strong demand for these types of materials in the marketplace. One of the key properties of PVP is its water solubility. This property can vary as a function of the molecular weight, but even very high molecular weight PVP is quite water-soluble. As demonstrated later, this attribute results in a PVP polymer film coating that is unable to resist water exposure for any length of time. Often, especially in paper and film-coating applications, original equipment manufacturers are under pressure to develop formulations improving the final product's ability to resist water. Recent developments, the details of

which are described elsewhere,<sup>2</sup> have led to a novel approach that considerably enhances the coating performance of PVP. These developments, broadly stated, are the intentional *in situ* incorporation of substantial amounts of insoluble PPVP nanoscale particles into soluble, film-forming PVP polymer, which results in an unusual molecular-scale composite structure that exhibits useful and unique properties in comparison with existing commercial PVP materials.

The focus of this report is to comprehensively present the first insights into the structure of molecular-composite poly(vinyl pyrrolidone) (MCPVP). Several methods suitable for measuring the components of this complex composite polymer system are identified, and typical results are presented. The work also aims to demonstrate the effect of significantly submicrometer, nanoscale particles on the viscoelastic and flow properties of a novel concentrated and aqueous polymeric solution. Finally, the work aims to demonstrate the utility of this film-forming molecular composite by demonstrating its improved and substantial ability to resist water penetration in an ink-jet printing application.

Correspondence to: D. K. Hood (dhood@ispcorp.com) or L. Senak (lsenak@ispcorp.com).

## EXPERIMENTAL

Poly(vinyl pyrrolidone),  $M_w \sim 1 \times 10^6$  g/mol (Grade K-90), was obtained from International Specialty Prod-

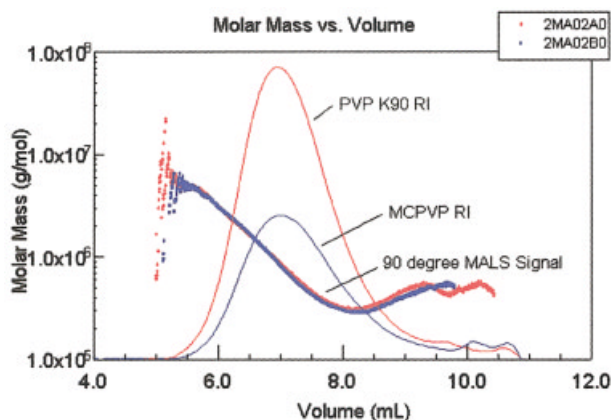


**Figure 1** Comparative GPC/MALS results for MCPVP (blue) and PVP K90 (red).

ucts (ISP) in Wayne, NJ. Molecular weight and weight fraction determination was performed with gel permeation chromatography (GPC)/multi-angle light scattering (MALS) instrumentation consisting of a Waters 590 solvent-delivery system (Milford, MA), a Waters 517 WISP autosampler, a single Shodex OH-PAK SB80-MHQ linear GPC column (SHOKO America Inc., Colorado Spring, CO), a Wyatt Technologies Dawn DSP MALS photometer (Santa Barbara, CA) equipped with a 632.8-nm laser, and a Waters 410 differential refractive-index detector set in tandem. The sample was first filtered through an Alltech 25-mm, 0.45- $\mu\text{m}$  nylon/glass syringe filter. The mobile phase used for these experiments was water/methanol (50/50 v/v) made 0.1M with  $\text{LiNO}_3$ . The flow rate was 0.5 mL/min. The injection volume for the analysis was 100  $\mu\text{L}$ . The polymer sample concentration was 0.15% (w/v) of the solid polymer to the mobile phase. All experiments were performed at 30°C. Data analysis was performed on Wyatt Technologies Astra software (version 4.5). The value of the polymer-specific refractive-index increment ( $dn/dc$ ) was measured for PVP with a Chromatix KMX-16 differential refractive-index detector (Sunnyvale, CA) using a 632.8-nm laser and was determined to be 0.175 mL/g.

Particle size determination with quasi-elastic light scattering (QELS) was accomplished with a Brookhaven Instruments 90 Plus (Holtville, NY). Measurements were made with a 50-mW laser at  $\lambda = 532$  nm. The scattering angle was 90°, and the temperature was 25°C. The samples were measured at 0.1% solids in water (0.1M salt) and passed through a 5- $\mu\text{m}$  filter before measurement.

Particle size determination with field flow fractionation (FFF)/MALS was accomplished with Wyatt Technology's AFFF system with a Dawn EOS laser (a 30-mW Ga-As laser at  $\lambda \sim 685$  nm) and an Optilab concentration detector. The scattering angle was 90° at a temperature of 25°C. The unfiltered sample was measured at 0.96 mg/mL in water. The mobile phase

was 100 mM  $\text{NaNO}_3$ , 200 ppm  $\text{NaN}_3$ , and water. The injection volume was 100  $\mu\text{L}$ .

The viscoelastic and flow properties of 11% solid solutions were determined with a TA Instruments AR1000N controlled stress rheometer (New Castle, DE) with a 4-cm cone with a 2° angle equipped with a solvent trap. Stress-mode oscillatory experiments were performed in the linear torque ramp mode from 0.1 to 10.0 Pa at a frequency of 1.0 rad/s. Controlled shear stress experiments were performed in the continuous ramp mode from 0.1 to 150.0 Pa. The ramp up/down time was 1 h. Both experiments required equilibration of the sample in the geometry for 10 min, and the temperature was kept at 25°C.

Atomic force microscopy (AFM) images were obtained on a Digital Instruments Nanoscope IIIa MultiMode (Woodbury, NY) operating in the tapping mode. Neat polymer films were cast by the solution being allowed to dry at room temperature, and then they were placed inside the ambient chamber for examination. Conventionally etched silicon probes (stiffness  $\sim 40$  N/m, resonant frequency = 160–170 kHz) were used.  $A_o$ , the amplitude of the freely oscillating probe, ranged from 10 to 30 nm. The set-point amplitude ranged from 0.5 $A_o$  to 0.8 $A_o$ .

## RESULTS AND DISCUSSION

The practical and theoretical considerations are well known for molecular weight determination by static light scattering.<sup>3</sup> GPC/MALS is an extension of light scattering studies in combination with GPC experiments and is well established for the molecular weight determination of PVP.<sup>4,5</sup> Absolute molecular weight information in light scattering experiments, across a molecular weight distribution in this case, is obtained from the intensity of the excess Rayleigh scattered light applied to the following equation:

$$K^*c/R_\theta = 1/M_w P(\theta) + 2A_2c \quad (1)$$

where  $R_\theta$  is the excess Rayleigh scattering ratio;  $c$  is the concentration of polymer molecules in solution;  $M_w$  is the polymer weight-average molecular weight;  $A_2$  is the polymer second virial coefficient; and  $P(\theta)$  is the theoretically derived form factor and is a function of the molecular  $z$ -average size, shape, and structure.  $K^*$  is the polymer solution optical constant:

$$K^* = 2\pi^2 n_0^2 (dn/dc)^2 \lambda_0^{-4} N_A^{-1} \quad (2)$$

where  $\lambda_0$  is the light scattering laser wavelength (632.8 nm),  $N_A$  is Avogadro's number,  $n_0$  is the refractive index for the mobile phase, and  $dn/dc$  is the polymer-specific refractive-index increment (or change of the refractive index with concentration). Therefore, with

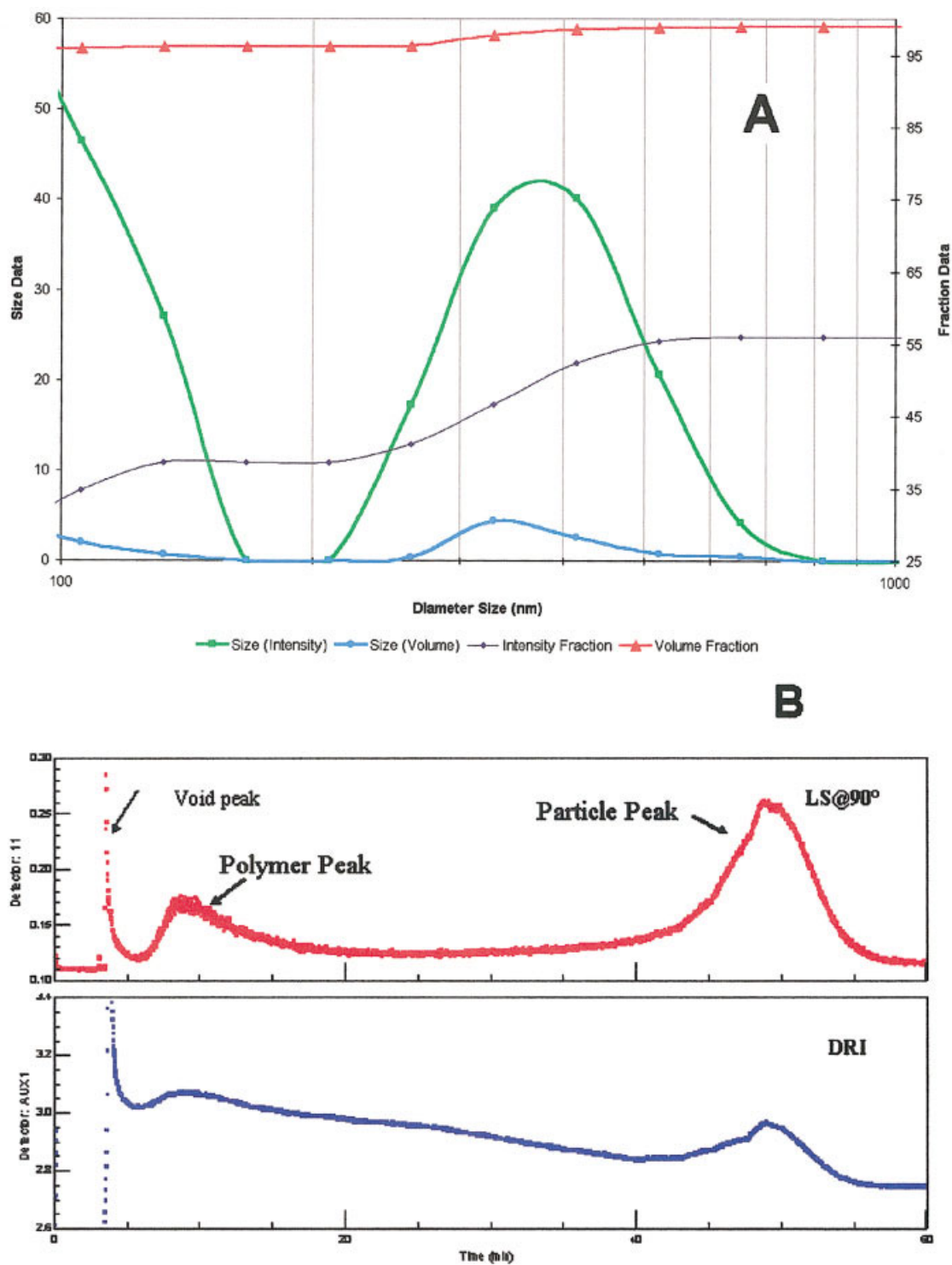


**Figure 2** (A) Typical QELS results for MCPVP [(■) size (intensity), (●) size (volume), (◆) intensity fraction, and (▲) volume fraction], (B) typical FFF chromatograms for MCPVP showing the MALS results (top) and the differential refractometer response (bottom), (C) Debye plot of the particulate fraction, and (D) MCPVP MALS results for the particulate fraction.

an established  $dn/dc$  value, the molecular weight and the concentration mass of the polymer eluting from the GPC column can be determined. Advantageously, from a known sample mass injected into the chromatographic system, a ratio of the eluted sample con-

centration to the original sample concentration can be determined readily. In other words, the weight fraction ( $\Phi$ ), or weight percentage, that is not soluble polymer may be calculated.  $\Phi$  may be expressed by the following relationship:

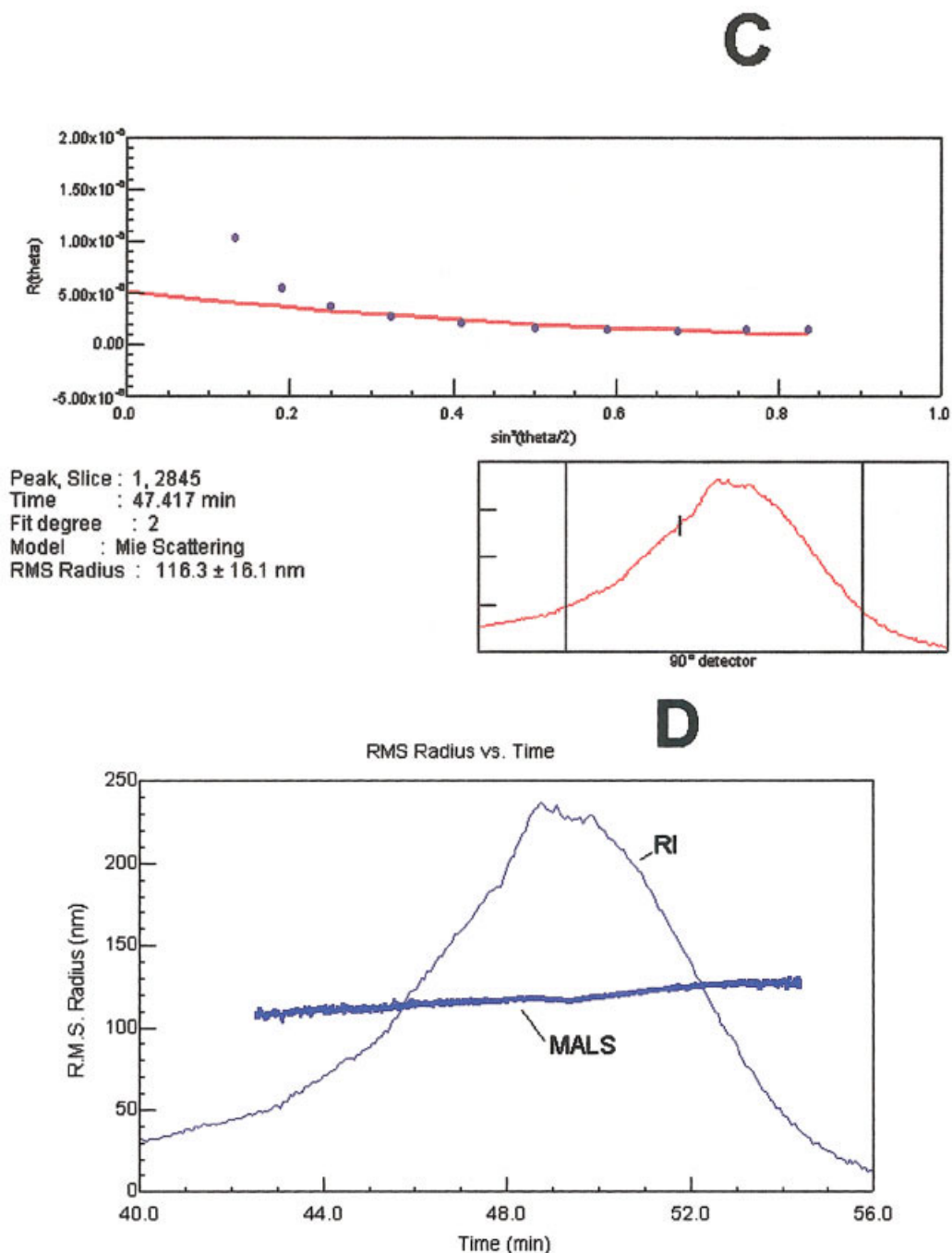


Figure 2 (Continued from the previous page)

$$\Phi = 1 - (W_f/W_t) \tag{3}$$

where  $W_t$  is the total polymer concentration by weight.  $W_f$  is the concentration, by weight, of the fraction of soluble polymer determined from the refractive-index detector response over the molecular weight distribution, as applied to eq. (1). For a completely recovered sample, this ratio is unity. For a sample in which not all of the material is soluble and the insoluble portion is filtered, the sample amount recovered will be some portion of the original sample

weight. Therefore, from the GPC/MALS experiment, not only are the sample's soluble structural features obtained, but the sample's compositional recovery may also be determined. Such methodology should only be considered semiquantitative because the possibilities of column adsorption and low molecular weight species eluting after the molecular weight distribution can cast doubt on the absolute values.

With this background in mind, typical results for the GPC/MALS experiment, in a comparative fashion, are presented for MCPVP and PVP K90 in Figure 1.

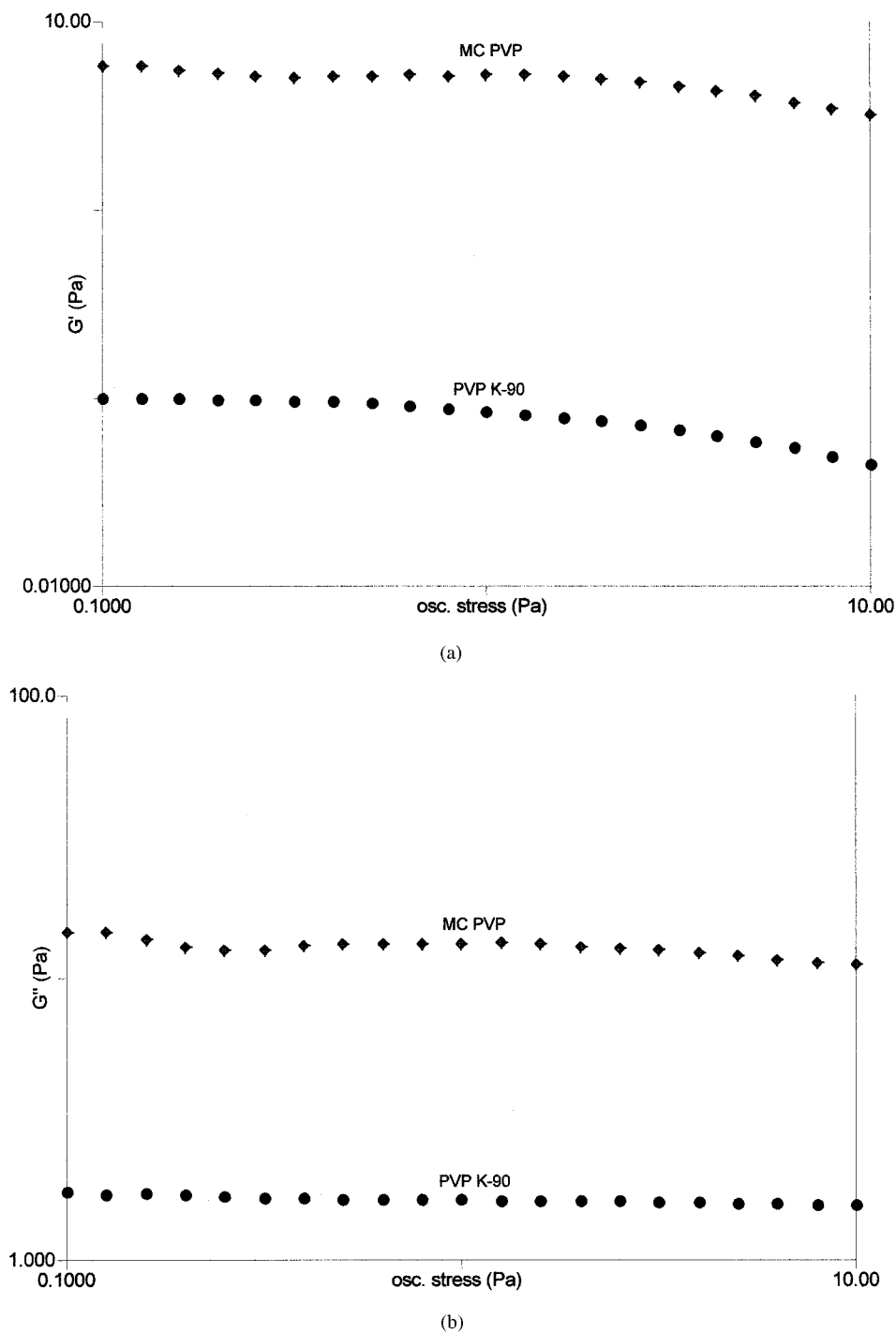


**Figure 3** Rheological profiles of MCPVP and PVP K90: (A)  $G'$ , (B)  $G''$ , (C)  $\tan \delta$ , and (D) viscosity versus the shear rate.

For equivalent injection concentrations and volumes, the differential refractometer indicates that the amount of soluble material differs by a factor of nearly two. Clearly, there is less soluble polymeric material in MCPVP. In fact, only about 51% of this MCPVP sample is soluble and recovered. Interestingly, the polymeric material that is soluble in MCPVP is structurally quite similar, in terms of the molecular weight and radius of gyration of the poly-

mer across the molecular weight distribution, to PVP K90. This point is confirmed by a very close overlay of the molar mass versus the retention volume. The continuity between the GPC behavior for MCPVP and PVP K90 demonstrates that the relationship between the retention volume and molecular weight is consistent for both soluble polymers or that the relationship between the molar mass and molecular size, as indicated by the retention vol-

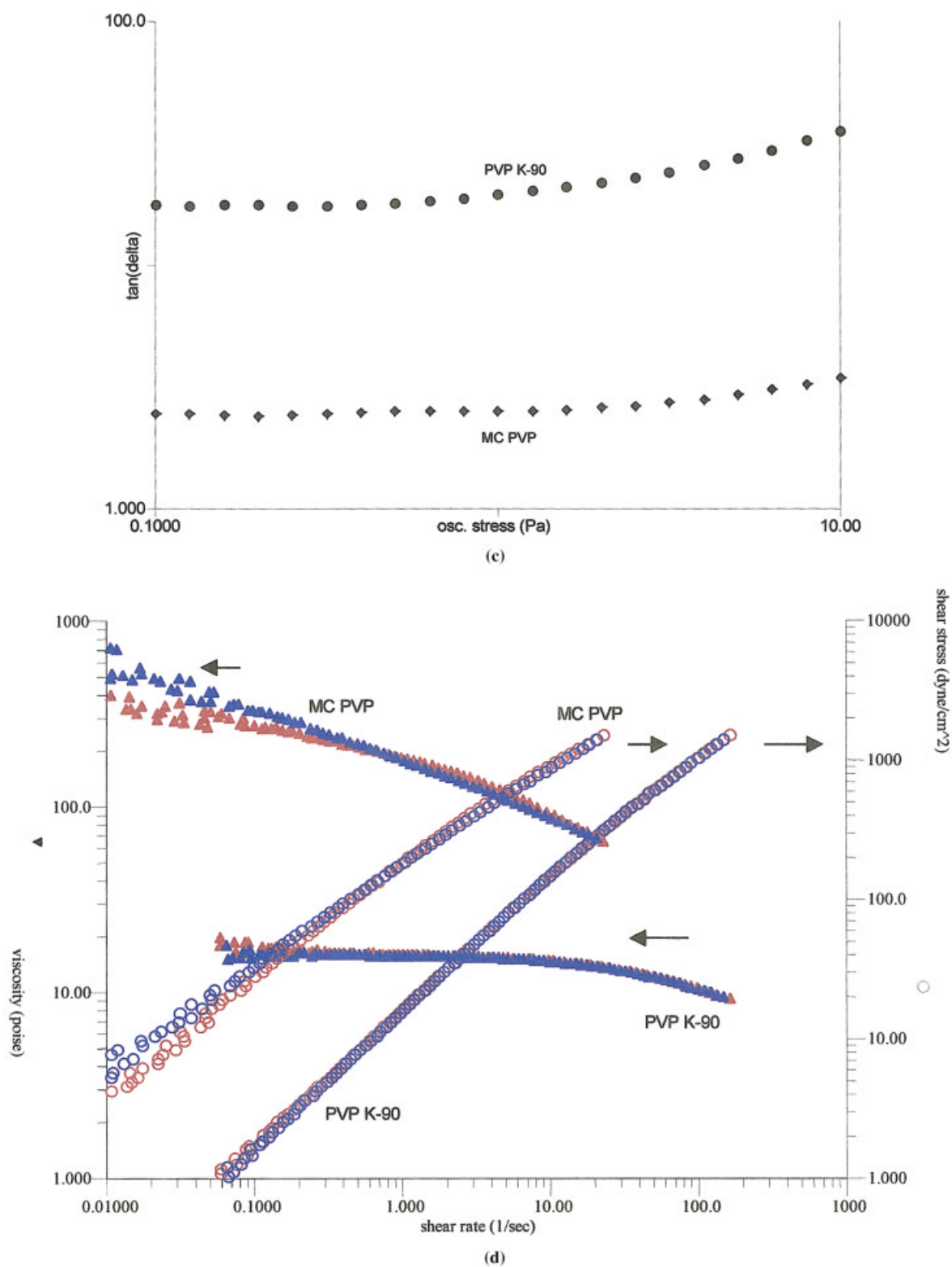
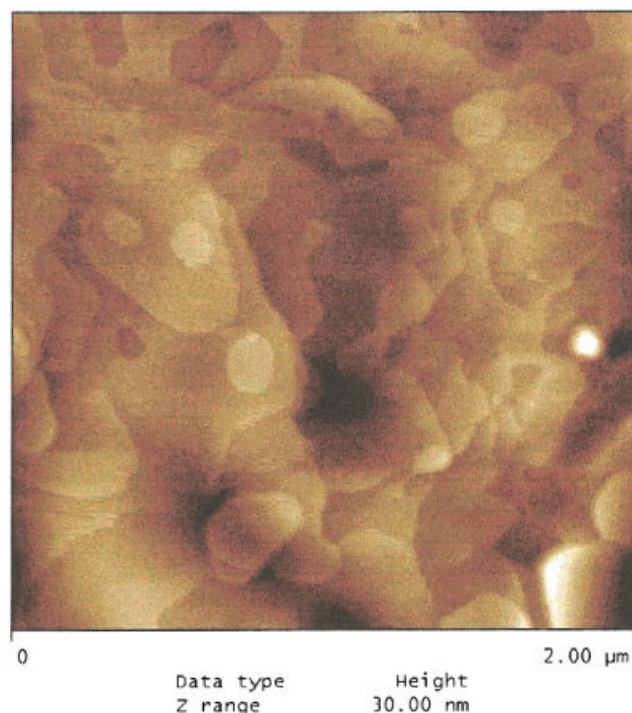


Figure 3 (Continued from the previous page)

ume, is identical. Therefore, the soluble polymers are conformationally very similar.

QELS results for MCPVP are presented in Figure 2(A). This figure represents the overall particle vol-

ume as a function of the diameter and provides a sense of its population. For PVP K90, no scattering is detected beyond approximately 150 nm (data not shown), and this defines the typical PVP soluble poly-



**Figure 4** AFM tapping-mode image: a height profile of a neat film of a nominally 50% insoluble MCPVP.

mer limit. In contrast, MCPVP reveals a distinct particle distribution, attributed to the insoluble particulate phase, which exhibits a diameter of approximately 370 nm. The results also suggest that there is a small amount of larger, micrometer-sized particles comprising a few percent of this distribution.

Asymmetric FFF/MALS results for MCPVP are presented in Figures 2(B–D). In Figure 2(B), the chromatograms illustrate two distinct peaks. The first peak is attributed to the soluble polymer, and the second peak is attributed to the insoluble polymer particle. Note that in this case, the differential refractive-index response is not necessarily indicative of the sample composition, in large part because of the differences in the refractive indices of the components. Upon massive dissolution, PVP typically forms a clear polymer solution. An MCPVP solution, however, becomes turbid because of the insoluble particulate fraction and its contribution to the overall refractive index of the solution. However, even with this, the results clearly demonstrate the two-phase nature of this system. FFF-MALS yields an insoluble polymer particle approximately 325 nm in diameter [Fig. 2(D), MALS curve], which is similar to the QELS result. At very low MALS angles [Fig. 2(C)], the increase in the angular dependence can be attributed to a small population of micrometer-sized particles. The resolution of this phenomenon is difficult under these experimental conditions. Note that these results are consistent with QELS, in that the insoluble particulate material is predominantly nanoscale.

It is well known that significantly submicrometer, nanoscale particles can have a dramatic effect on the rheology of a polymeric solution or fluid.<sup>6–10</sup> Such particulate systems are capable of demonstrating increased structure, enhanced shear thinning, and even shear thickening (dilatant) behavior. The effects are primarily attributed to the formation of a secondary structure within a fluid. Among some of the critical parameters identified as capable of inducing additional structural effects are the dispersed particle volume fraction, particle size distribution, particle shape, continuous phase viscosity, and fluid flow field. Therefore, as expected, the presence of these nanoscale PPVP particles in the MCPVP fluid results in a significant increase in the magnitude of the storage modulus ( $G'$ ) and loss modulus ( $G''$ ), whereas  $\tan \delta$ , a measure of the overall elasticity of the system, decreases substantially [Fig. 3(A–C)]. The nature of the system transitions from a primarily viscous fluid to a more rigid and strongly elastic fluid. Continuous flow tests indicate that MCPVP exhibits a much greater viscosity coupled to strong shear thinning behavior, where  $n$  is less than 1 for a power-law fit, in comparison with a similar PVP K90 fluid [Fig. 3(D)]. This pseudoplastic behavior is a clear indication of the structure within the fluid that collapses under flow. At low shear rates, there is little sign of the viscosity leveling or a plateau. In contrast, PVP K90 exhibits a nearly Newtonian behavior to  $10 \text{ s}^{-1}$ . There are subtle signs of thixotropy, time-dependent viscosity behavior, in MCPVP. We have seen for similar systems, where  $\Phi$  approaches 75%, that introducing substantial thixotropic behavior is possible.<sup>11</sup>

Atomic force microscopy (AFM) results presented in Figure 4 indicate a massive and distributed hetero-

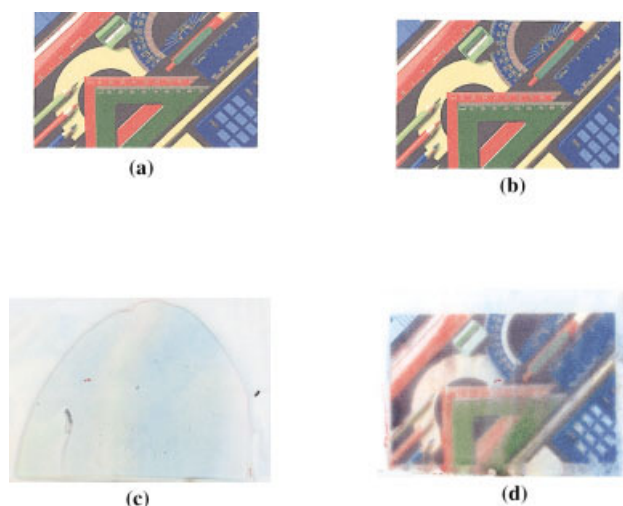


**Figure 5** Ink-jet printing application test: (A) PVP K90 before the test, (B) PVP K90 after 5 min of submersion in 25°C water, (C) MCPVP before the test, and (D) MCPVP after 5 min of submersion in 25°C water.

geneity in the material.<sup>12</sup> Presented is a typical result for the height image or topography of the polymer film. In general, as the color becomes lighter, the elevation of the sample increases. On the 2- $\mu\text{m}$  scale field of view, substantial differences in the composition of MCPVP are readily apparent. The physical structure of this image appears as a snake-skin type of MCPVP accompanied by evidence of very fine particulate matter. A possible explanation of the scalelike structure is that as the polymer solution dries, the PPVP particles undergo some agglomeration. Further work is required to fully understand this behavior. However, it is important to note that unlike typical PVP, which at this scale is completely featureless, this material exhibits substantial additional physical structure on a submicrometer scale.

To illustrate the unique performance of MCPVP, we performed a typical ink-jet print quality test. A neat, nominally 11% solution of MCPVP or PVP K90 of a molecular weight grade ( $M_w$  was nominally  $1.0\text{--}1.5 \times 10^6$  g/mol) was cast as a film, with a #38 Meyer rod, onto DuPont-Teijin Melanex polyester film. The resulting dry coating thickness was approximately 9  $\mu\text{m}$ . This wet coating was dried in a 90°C air oven for 10 min. Images were printed onto the film coating with a Hewlett-Packard HP950C Deskjet printer set for the HP Premium Photo Paper glossy mode (Palo Alto, CA). After standing overnight, the images were submerged in water for 5 min. The results of this experiment are illustrated in Figure 5. The PVP K90 image is completely dissipated [Fig. 5(B)] and unrecognizable, whereas, although there has been some image quality deterioration for MCPVP, the image is still easily recognizable [Fig. 5(D)]. For MCPVP, the matrix formed by the molecular entanglements of dried, soluble PVP and insoluble PPVP dampens its ability to solvate and redisperse. Therefore, MCPVP exhibits a tremendous improvement in dye/image retention and water fastness. We have observed similar beneficial effects for other copolymeric molecular composites, such as those of vinyl pyrrolidone and *N*-[3-(dimethylamino)propyl]methacrylamide. Again, it is important to note this film formation is reversible and that MCPVP will eventually completely redisperse into solution.

## CONCLUSIONS

The coupling of different components, soluble and insoluble, into MCPVP has a tremendous impact on

the macroscopic properties, whether in solution or in the solid state. A variety of analytical methods have been identified as suitable for characterizing this new molecular-composite structure. Light scattering techniques indicate that the bulk of the insoluble particulate matter is in the range of 300–400 nm. In the fluid state, the polymeric solution is much more elastic and structured, especially in comparison with PVP nominally having an  $M_w$  value of  $1 \times 10^6$  g/mol. This is due to the nanoscale PPVP particles and the additional structure formed by these particles in the solution. This physical structure, when translated into a solid film coating, demonstrates a substantial improvement in water resistance. Although only one narrow application has been explored, this material clearly has wide-ranging possibilities. From its potential for new vehicles for delivering poorly water-soluble compositions to improved film performance for a wide variety of substrates, this polymeric composite introduces substantial and new possibilities for vinyl pyrrolidone polymer chemistry through the unique modification of its chemical architecture.

The authors thank John Inderdonen, Jean Luc Bruseau, and Bruce Weiner of Brookhaven Instruments for performing QELS measurements, Michelle Chen of Wyatt Technology for performing FFF/MALS experiments, Sergei Magonov of Digital Instruments for the AFM image used in this publication, and the management of International Specialty Products for the opportunity to publish this work.

## References

1. Barabas, E. In *Encyclopedia of Polymer Science and Engineering*; Mark, H. F., Ed.; Wiley-Interscience: New York, 1989; Vol. 17, p 198.
2. Hood, D. K.; Kopolow, S. L.; Tallon, M.; Kwak, Y. T.; Senak, L.; Patel, D.; McKittrick, J. PCT IPN WO02/22722 A1 (2002).
3. Zimm, B. *J Chem Phys* 1948, 16, 1093.
4. Xu, Y.; Teraoka, I.; Senak, L.; Wu, C.-S. *Polymer* 1999, 40, 7359.
5. Senak, L.; Wu, C.-S.; Malawer, E. G. *J Liq Chromatogr* 1987, 10, 1127.
6. Laun, H. M. *Angew Makromol Chem* 1984, 123, 335.
7. Barnes, H. A. *J Rheol* 1989, 33, 329.
8. Bender, J.; Wagner, N. J. *J Rheol* 1996, 40, 899.
9. Ferry, J. D. *Viscoelastic Properties of Polymers*, 2nd ed.; Wiley: New York, 1970.
10. Macosko, C. W. *Rheology*; Wiley: New York, 1994.
11. Hood, D. International Specialty Products internal unpublished report, 2000.
12. Magonov, S. N. In *Encyclopedia of Analytical Chemistry*; Meyer, R. A., Ed.; Wiley: Chichester, England, 2000; p 7432.